

Developments of Raman spectroscopy in the past 40 years: from a molecule to a living cell

Hiro-o Hamaguchi

Department of Chemistry, School of Science, The University of Tokyo, 7-3-1 Hongo, Bunkyo-ku, Tokyo 113-0033, Japan, and
Institute of Molecular Science and Department of Applied Chemistry, National Chiao Tung University, 1001 Ta Hsueh Road, Hsinchu, Taiwan 300

This article is based on the opening lecture ‘Raman spectroscopy at Tokyo: past 40 years and future’ delivered at the symposium entitled ‘80 years of Raman effect: reflections and the future’ held at Bangalore from 8 to 10 December 2008. It reviews four research subjects, including (1) anomalous depolarization ratios in resonance Raman scattering, (2) one-way photoisomerization of retinal by nanosecond time-resolved Raman spectroscopy, (3) dynamic polarization model of photoisomerization of stilbene by picosecond time-resolved Raman spectroscopy, and (4) discovery of the ‘Raman spectroscopic signature of life’ by time- and space-resolved Raman spectroscopy. The future possibilities of Raman spectroscopy are also briefly addressed.

Keywords: Anomalous depolarization ratio, photoisomerization, Raman scattering, yeast cells.

Introduction

THE discovery of the Raman effect is undoubtedly one of the greatest scientific achievements in the last century¹. It originated from India, but fast spread all over the world. As a result, Raman was awarded a Nobel Prize in 1930, also surprisingly quickly, only two years after his discovery. Raman spectroscopy was introduced in Japan in the early 1930s and played a crucial role in the discovery of the rotational isomerism (*trans* and *gauche*) of the C–C single bond by Mizushima and co-workers^{2,3}. This discovery was an immediate and distinct product of Raman spectroscopy that was followed by many others.

Since the early 1930s, there has been a long tradition of Raman spectroscopy at the Department of Chemistry, School of Science, The University of Tokyo. The present author did his first Raman experiment in 1968, 40 years after Raman’s discovery, in the laboratory of Takehiko Shimanouchi. The laboratory had a newly constructed laser Raman spectrometer as well as an old, traditional Raman spectrograph with a large mercury lamp. An NEC He–Ne laser, a Spex double monochromator and a Hamamatsu photomultiplier were utilized with a laboratory-made lock-in amplifier using bulbs. It took tens of minutes to scan a Raman spectrum, several orders of mag-

nitude longer than it does today, with a multichannel Raman spectrometer.

Since 1968, the present author has been involved in basic research in Raman spectroscopy, and has witnessed several dramatic developments in the field, viz. resonance Raman spectroscopy, nanosecond and picosecond time-resolved Raman spectroscopy, nonlinear Raman spectroscopy, and time- and space-resolved Raman spectroscopy. He has always been fascinated by the width and depth that Raman spectroscopy has to offer. In the following, four topics from his research activities in the past 40 years have been selected and described.

Anomalous depolarization ratios in resonance Raman scattering (1970s)

In textbooks on Raman spectroscopy, it is often (almost always) stated that the depolarization ratio ρ for linearly polarized light takes the value $0 \leq \rho < 0.75$ for totally symmetric vibrations and $\rho = 0.75$ for non-totally symmetric vibrations. This statement, however, is valid only when the Placzek polarizability theory holds. Placzek⁴ showed that (1) if the exciting radiation is off resonant from the electronic transitions of the molecule (off-resonant condition) and (2) if the ground electronic state is non-degenerate (non-degenerate condition), a Raman scattering tensor component $\alpha_{\rho\sigma}$ is, in a good approximation, given by the vibrational matrix element of a polarizability tensor component $\langle v' | \alpha_{\rho\sigma} | v'' \rangle$. Under these conditions, the Raman scattering tensor is always symmetric because the polarizability tensor is always symmetric from its definition. Then, among the three rotational invariants G_0 (trace), G_a (anti-symmetric) and G_s (symmetric) of the Raman scattering tensor, G_a vanishes and only G_0 and G_s can have non-zero values. Thus $0 \leq \rho = (5G_a + 3G_s)/(10G_0 + 4G_s) \leq 0.75$ holds. Placzek pointed out that if either of the above two conditions is not satisfied, the polarizability theory does not hold any more and that the Raman scattering tensor can become asymmetric having a non-zero anti-symmetric part, G_a . In this case, ρ can take any value between zero and infinity. Placzek even predicted that such a breakdown of the polarizability theory was likely to happen for an a_{2g} vibration of a D_{4h} molecule. The prediction was indeed verified by Spiro and Strekas in 1972, when they found what they

e-mail: hhama@chem.s.u-tokyo.ac.jp

called 'anomalous' depolarization ratios in the resonance Raman spectra of ferrocytochrome *c* and haemoglobin⁵. Several a_{2g} vibrations of the heme ring (approximately D_{4h} symmetry) showed depolarization ratios much larger than 0.75, values that were never expected from the polarizability theory and were thus called 'anomalous'.

With regard to the second assumption (non-degenerate condition), a clear example of the breakdown of the polarizability theory was given by the present author^{6,7} for the hexachloroiridate (IV) IrCl_6^{2-} and the hexabromoiridate (IV) IrBr_6^{2-} ions. These ions have ground electronic states with E_g'' symmetry, which is doubly degenerate (Kramers doublet) in the spin-orbit space. A set of polarized resonance Raman spectra of IrBr_6^{2-} is shown in Figure 1, in which all the observed Raman bands show depolarization ratio of unity⁶. This unusual result is not due to an experimental mistake, but is a consequence of the ground state electronic degeneracy.

Because the ground electronic state has two degenerate sublevels, α and β , any vibrational transition consists of four degenerate vibronic transitions designated by $\alpha \rightarrow \alpha$, $\alpha \rightarrow \beta$, $\beta \rightarrow \alpha$, $\beta \rightarrow \beta$. For example, the $\nu = 0 \rightarrow \nu = 1$ transition of ν_1 (a_{1g} symmetry) consists of four transitions: $\tilde{\alpha}_0 \rightarrow \alpha_1$, $\tilde{\alpha}_0 \rightarrow \beta_1$, $\tilde{\beta}_0 \rightarrow \alpha_1$, $\tilde{\beta}_0 \rightarrow \beta_1$. The symmetry of the Raman scattering tensor is given by the direct product $(E_g'' \times a_{1g}) \times (E_g'' \times a_{1g}) = A_{1g} + T_{1g}$. It contains not only a totally symmetric A_{1g} component, but also an anti-symmetric T_{1g} component. If we assume resonance with an excited state with E_u'' symmetry (and this is the case with the 568.2 nm excitation), we can group-theoretically calculate the four patterns of the Raman scattering tensor for the ν_1 fundamental transition⁷. The results are shown in Figure 2, with the corresponding values of rotational invariants. Since the four transitions occur independently without any phase relations, we simply add up these invariants to obtain $G_0 = 6$, $G_a = 12$ and $G_s = 0$. The depolarization ratio then becomes $\rho = (3G_s + 5G_a)/(10G_0 + 4G_s) = 1$, as observed in Figure 2.

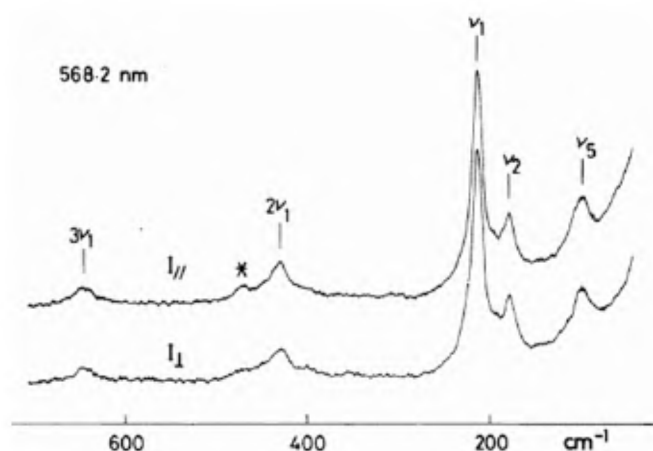


Figure 1. Polarized resonance Raman spectra of the hexabromoiridate (IV) ion.

In this way, as already reviewed⁸, the polarization characteristics of Raman scattering considered by Placzek had been fully elucidated experimentally by 1976.

One-way photoisomerization of retinal by nanosecond time-resolved Raman spectroscopy (1980s)

Toward the end of the 1970s, Raman spectroscopists began the challenge of measuring short-lived reaction intermediates. This challenge was facilitated by resonance Raman spectroscopy developed in the preceding decade; resonance enhancement was found essential in detecting low-concentration, short-lived intermediate species. Thus the term TR³, i.e. time-resolved resonance Raman was invented. Following the pioneering work by Wilbrandt and co-workers⁹, a number of photochemical intermediates were studied using nanosecond time-resolved Raman spectroscopy^{10,11}.

In Tokyo, time-resolved Raman spectroscopy started with the introduction of a quanta-ray Q-switched Nd:YAG laser. We constructed a nanosecond time-resolved Raman system based on this laser source with a Spex Triplemate spectrometer, an EG&G PAR intensified diode array and a DEC MINC mini-computer. The first sample was *trans*-stilbene. We were successful in obtaining a spectrum of S_1 *trans*-stilbene, whose lifetime is less than 100 ps, though we used nanosecond laser pulses. Our results¹² were published in 1983, but were preceded by Gustafson and co-workers¹³, who reported picosecond Raman spectra of the S_1 *trans*-stilbene a few months earlier.

Retinal is a prototype molecule both in photochemistry and photobiology. It exhibits *trans/cis* photoisomerization. One unusual aspect of retinal photoisomerization is that the *cis* to *trans* conversion is efficient, but the reverse *trans* to *cis* isomerization is much less efficient, as shown in Figure 3. This asymmetric photoisomerization of retinal is in contrast with the common symmetric

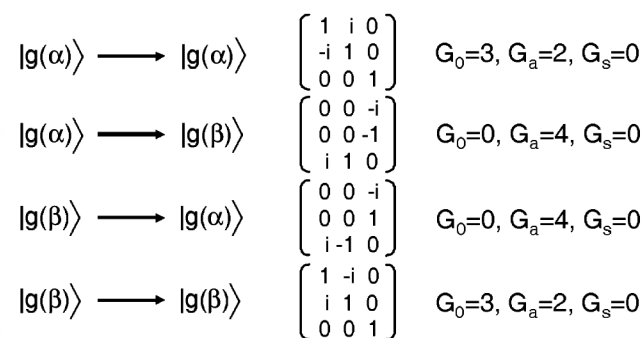
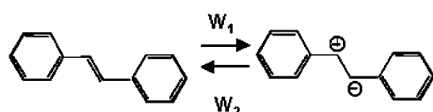


Figure 2. Four patterns of Raman scattering tensor for the ν_1 fundamental transition of MX_6 in the E_g'' ground electronic state in resonance with an E_u'' excited electronic state.

Fourier-transform limited apparatus, accurate band-shape analysis was possible. In order to understand the solvent-dependent band-shape changes and their relationship with isomerization, we introduced a model in which the C=C stretch frequency was stochastically modulated by the time-dependent polarization of the S_1 state (termed dynamic polarization)^{19,20}. According to this model, the fluctuation of the solvent field affects the energy gap between the S_1 and a nearby polarized state and hence this polarized state is occasionally mixed into the S_1 state. The C=C stretch frequency then changes stochastically between the two limiting values, the C=C double-bond frequency ω_1 in the S_1 state and the C⁺–C[–] single-bond frequency ω_2 in the polarized state ($\omega_1 > \omega_2$).



The band shape under such dynamic exchange was formulated for a limiting case²¹ in which the forward hopping rate W_1 is much smaller than the backward hopping rate W_2 . Using this formulation, we were able to fit the observed band shapes well (Figure 6).

It was further found that the forward hopping rate W_1 obtained by the fitting correlated linearly with the isomerization rate. We thus proposed a model (dynamic polarization model) for the photoisomerization of *trans*-stilbene²⁰, which involves the hopping to the polarized state as the requisite primary step (Figure 7). This model

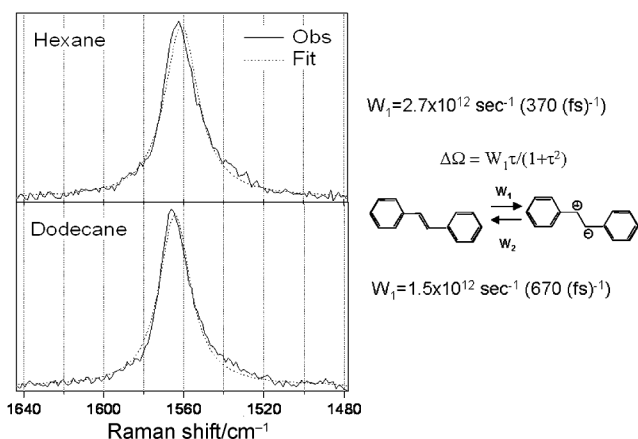


Figure 6. Band-fitting of the C=C stretch band based on the dynamic polarization model.

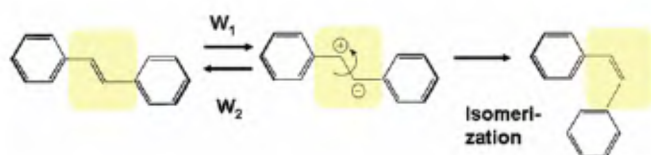


Figure 7. Dynamic polarization model of photoisomerization of S_1 *trans*-stilbene.

provides a new molecular-level view on chemical reactions in solution, with details on when, why and how they proceed.

Time- and space-resolved Raman spectroscopy of living yeast cells: the discovery of the ‘Raman spectroscopic signature of life’ (2000s)

We started work on a new topic of Raman spectroscopy in the year 2000 – time-resolved Raman spectroscopy of photochemical reaction intermediates evolved into time- and space-resolved Raman spectroscopy of living cells. We focused on yeast cells, in particular fission yeast (*Schizosaccharomyces pombe*), which is a well-known model cell for various biochemical studies. It divides symmetrically according to the cell cycle $G2 \rightarrow M \rightarrow G1 \rightarrow S \rightarrow G2$, just as cells in higher organisms do.

We were able to make the first observation of Raman spectral changes during mitosis²². Figure 8 shows the time- and space-resolved Raman spectra of a dividing fission yeast cell. We started the Raman measurement from the early M phase (0 min), in which a dividing nucleus was observed at the centre of the cell. At 11 min, the two nuclei were put apart symmetrically. At 31 min (G1/S phase), the nuclei were completely separated and located at the two ends of the cell. In the following S stage, a septum started to form from the plasma membrane (41 min). Finally, the septum became mature at 62 min and two daughter cells were formed. During mitosis, the Raman spectrum changes drastically. The Raman bands at 0 min are assigned to the proteins in the nucleus. The spectrum at 6 min is a superposition of those of the mitochondrion and cytoplasm. It means that the mitochondria are generated at the central part of the cell. At 11–31 min,

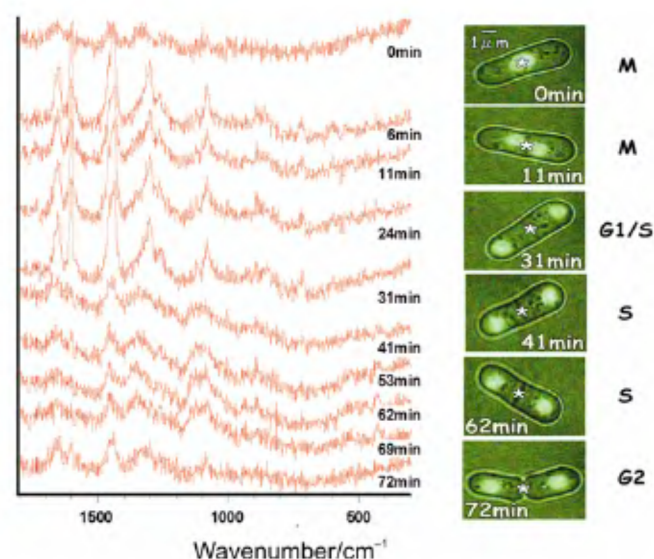


Figure 8. Time- and space-resolved Raman spectra from a dividing yeast cell.

the phospholipid bands from mitochondria are observed dominantly with a strong and sharp unknown band at 1602 cm^{-1} . This band was strong when the yeast cell was in a good nutritious condition, but became weak without nutrients. After 41 min, the Raman spectra are dominated by the bands of polysaccharides in the septum and cell wall.

In order to study in further detail the relationship between the band intensity at 1602 cm^{-1} and cell activity, we added KCN to the yeast cell sample, in order to study the effect of respiration inhibition on the intensity of the 1602 cm^{-1} band^{23,24}. The time- and space-resolved Raman spectra of a KCN-treated yeast cell are shown in Figure 9.

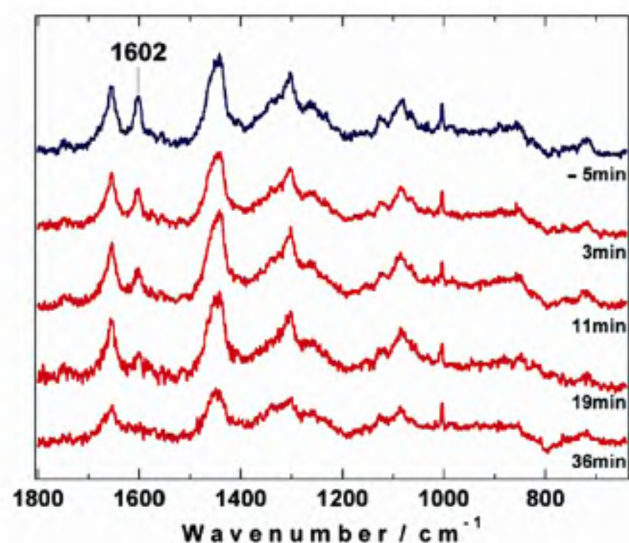


Figure 9. Time- and space-resolved Raman spectra of a single fission yeast cell treated with KCN.

The time resolution of the experiment was 100 s. Five minutes before the addition of KCN, the Raman spectrum shows a strong band at 1602 cm^{-1} with prominent phospholipid bands at 1655 , 1446 and 1300 cm^{-1} . Three minutes after addition of KCN, the intensity of 1602 cm^{-1} band decreases considerably, while the other phospholipid bands remain unchanged. As time goes on, the 1602 cm^{-1} band becomes weaker and finally disappears at 36 min. Concomitantly, the phospholipid bands gradually change from the well-resolved peaks to diffuse, broad bands. We consider the effect of KCN in two steps. First, cellular respiration is inhibited by KCN and the metabolic activity of the mitochondria is lowered. This process is most probably monitored by the intensity of the 1602 cm^{-1} band. Second, the double-membrane structure of the mitochondria is degraded by the lowered metabolic activities, and it is eventually destroyed. This process has been probed by the changes in the phospholipid bands. It is highly likely that the 1602 cm^{-1} band probes the primary dying process of the KCN-treated yeast cell through the metabolic activity of the mitochondria. We call this band the 'Raman spectroscopic signature of life'.

The use of the 'Raman spectroscopic signature of life' will lead to a real non-invasive and *in vivo* diagnostics of the viability of a single living cell.

Future perspective

It is certain that the time and space specificity of Raman spectroscopy is being more and more appreciated in various fields of application. It will most probably be best appreciated in biomedical applications in which, as

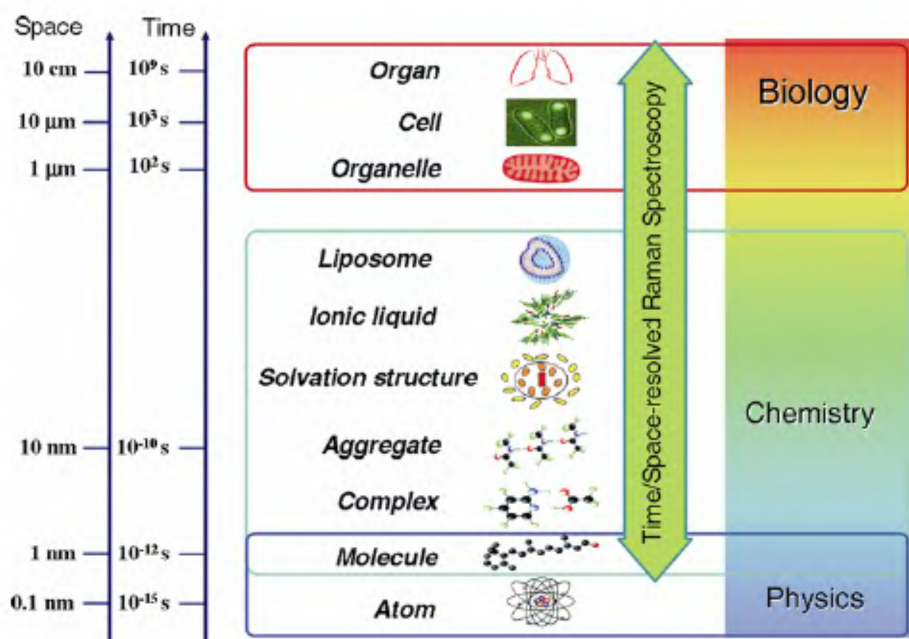


Figure 10. Time- and space-resolved Raman spectroscopy.

pointed out by Schrödinger²⁵, time- and space-specific biological events can only be accounted for by physics and chemistry, and Raman spectroscopy is the only presently available physico-chemical method for this line of approach to life. Raman spectroscopy will be used even more extensively than it is now, with its applications covering the whole material world starting from a molecule to a single cell and a human organ (Figure 10).

1. Raman, C. V. and Krishnan, K. S., A new type of secondary radiation. *Nature*, 1928, **121**, 501.
2. Mizushima, S., Morino, Y. and Higashi, K., *Sci. Papers Inst. Phys. Chem. Res.*, 1934, **25**, 159.
3. Mizushima, S., Morino, Y. and Noziri, S., Raman effect and free rotation. *Nature*, 1936, **137**, 945.
4. Placzek, G., In *Handbuch der Radiologie*, Akademische Verlagsgesellschaft, Leipzig, 1934, vol. 6, p. 208.
5. Spiro, T. G. and Strekas, T. C., Resonance Raman spectra of hemoglobin and cytochrome *c*: inverse polarization and vibronic scattering. *Proc. Natl. Acad. Sci. USA*, 1972, **69**, 2622–2626.
6. Hamaguchi, H. and Shimanoouch, T., Anomalous polarization in the resonance Raman effect of the octahedral hexabromoiridate(IV) ion. *Chem. Phys. Lett.*, 1976, **38**, 370–373.
7. Hamaguchi, H., Group-theoretical study on the Raman tensor patterns in vibrational resonance Raman scattering: application to the hexabromoiridate (IV) ion. *J. Chem. Phys.*, 1977, **66**, 5757–5768.
8. Hamaguchi, H., In *Advances in Infrared and Raman Spectroscopy* (eds Clark, R. J. H. and Hester, R. E.), Wiley Heyden, Chichester, 1985, vol. 12.
9. Pagsberg, P., Wilbrandt, R., Hansen, K. B. and Weinberg, K. V., Fast resonance Raman spectroscopy of short-lived radicals. *Chem. Phys. Lett.*, 1976, **39**, 538–541.
10. Atkinson, G. H., In *Advances in Infrared and Raman Spectroscopy* (eds Clark, R. J. H. and Hester, R. E.), Wiley Heyden, Chichester, 1982, vol. 9.
11. Hamaguchi, H., In *Vibrational Spectra and Structure* (ed. Durig, J. R.), Elsevier, Amsterdam, 1987, vol. 16.
12. Hamaguchi, H., Kato, C. and Tasumi, M., Observation of transient resonance Raman spectra of the S_1 state of *trans*-stilbene. *Chem. Phys. Lett.*, 1983, **100**, 3–7.
13. Gustafson, T. L., Roberts, D. M. and Chernoff, D. A., Picosecond transient Raman spectroscopy: the photoisomerization of *trans*-stilbene. *J. Chem. Phys.*, 1983, **79**, 1559–1564.
14. Hamaguchi, H., Okamoto, H., Tasumi, M., Mukai, Y. and Koyama, Y., Transient Raman spectra of the all-*trans* and 7-, 9-, 11- and 13-mono-*cis* isomers of retinal and the mechanism of the *cis-trans* isomerization in the lowest excited triplet state. *Chem. Phys. Lett.*, 1984, **107**, 355–359.
15. Arai, T., Karatsu, T., Sakuragi, H. and Tokumaru, K., ‘One-way’ photoisomerization between *cis*- and *trans*-olefin. A novel adiabatic process in the excited state. *Tetrahedron Lett.*, 1983, **24**, 2873–2876.
16. Tahara, T., Toleutaev, B. N. and Hamaguchi, H., Picosecond time-resolved multiplex coherent anti-Stokes Raman scattering spectroscopy by using a streak camera: isomerization dynamics of all-*trans* and 9-*cis* retinal in the lowest excited triplet state. *J. Chem. Phys.*, 1994, **100**, 786–796.
17. Yamaguchi, S. and Hamaguchi, H., Femtosecond ultraviolet-visible absorption study of all-*trans* \rightarrow 13-*cis* 9-*cis* photoisomerization of retinal. *J. Chem. Phys.*, 1998, **109**, 1397–1408.
18. Iwata, K., Yamaguchi, S. and Hamaguchi, H., Construction of a transform-limited picosecond time-resolved Raman spectrometer. *Rev. Sci. Instrum.*, 1993, **64**, 2140–2146.
19. Hamaguchi, H. and Iwata, K., Exchange model of vibrational dephasing in S_1 *trans*-stilbene in solution and its possible correlation with the isomerization reaction. *Chem. Phys. Lett.*, 1993, **208**, 465–470.
20. Hamaguchi, H. and Iwata, K., Physical chemistry of the lowest excited singlet state of *trans*-stilbene in solution as studied by time-resolved Raman spectroscopy. *Bull. Chem. Soc. Jpn.*, 2002, **75**, 883–897.
21. Hamaguchi, H., Solvent-induced dynamic polarization and vibrational dephasing of electronically excited molecules. *Mol. Phys.*, 1996, **89**, 463–471.
22. Huang, Y.-S., Karashima, T., Yamamoto, M. and Hamaguchi, H., Molecular-level pursuit of yeast mitosis by time- and space-resolved Raman spectroscopy. *J. Raman Spectrosc.*, 2003, **34**, 1–3.
23. Huang, Y.-S., Karashima, T., Yamamoto, M., Ogura, T. and Hamaguchi, H., Raman spectroscopic signature of life in a living yeast cell. *J. Raman Spectrosc.*, 2004, **35**, 525–526.
24. Huang, Y.-S., Karashima, T., Yamamoto, M. and Hamaguchi, H., Molecular-level investigation of the structure, transformation and bioactivity of single living fission yeast cells by time- and space-resolved Raman spectroscopy. *Biochemistry*, 2005, **44**, 10009–10019.
25. Schrödinger, E., *What is Life?* Cambridge University Press, Cambridge, 1944.

ACKNOWLEDGEMENT. I am grateful to the many collaborators during the work described here.